Int J Thermophys (2010) 31:1131–1144
DOI 10.1007/s10765-010-0839-0

Molecular Dynamics Modeling of Latent Heat Enhancement in Nanofluids

Muhsin M. Ameen · K. Prabhul · G. Sivakumar · Praveen P. Abraham · U. B. Jayadeep · C. B. Sobhan

Received: 19 December 2009 / Accepted: 24 September 2010 / Published online: 8 October 2010

Abstract A discrete computational approach based on molecular dynamics (MD) simulations is proposed for evaluating the latent heat of vaporization of nanofluids. The computational algorithm, which considers the interaction of the solid and the fluid molecules, is used for obtaining the enhancement of the latent heat of a base fluid due to the suspension of nanoparticles. The method is validated by comparing the computed latent heat values of water with standard values at different saturation temperatures. Simulation of a water–platinum nanofluid system is performed, treating the volume fraction and size of nanoparticles as parameters. The trends in the variation are found to match well with experimental results on nanofluids. Discussions are also presented on the limitations of the proposed model, and on methods to overcome them.

Keywords Latent heat · Molecular dynamics · Nanofluids

M. M. Ameen · K. Prabhul · G. Sivakumar · P. P. Abraham
Nanotechnology Research Laboratory, National Institute of Technology Calicut, Calicut 673 601, Kerala, India

U. B. Jayadeep · C. B. Sobhan
Department of Mechanical Engineering, National Institute of Technology Calicut, Calicut, India

C. B. Sobhan (✉)
School of Nano Science and Technology, National Institute of Technology Calicut, Calicut, India
e-mail: csobhan@nitc.ac.in

List of Symbols

d_{NP}	Effective outer diameter of the nanoparticles
e	Total energy
L	Box length
m	Mass, kg
N_p	Number of atoms in the nanoparticles
P	Pressure
p(t)	Present pressure
P_o	Desired pressure
r	Inter-atomic distance, m
$r_{c.m}$	Position of the center of mass of the nanoparticles
R_g	Radius of gyration
t	Time
T	Temperature
T_o	Desired temperature
v	Velocity

Greek Symbols

μ	Pressure scaling factor
β	Isothermal compressibility factor
ε	Minimum value of $\phi_{LJ,J}$
σ	Inter-atomic distance at which $\phi_{LJ} = 0$, nm
τ_p	Time constant
ϕ	Inter-atomic potential, J

Subscripts

O–O	oxygen–oxygen
O–Pt	oxygen–platinum
H–Pt	hydrogen–platinum
i	ith particle
j	jth particle

1 Introduction

Being a very effective method of heat removal, a liquid–vapor phase change has been attracting immense attention as a research problem. Examples of the applications of phase-change heat transfer cover a wide spectrum, ranging from direct thermal control of microelectronics to passive heat transfer devices such as heat pipes and micro-heat pipes [1]. High rates of heat transfer in the form of latent heat and the constancy of temperature during the process make phase-change heat transfer a preferred option for achieving the two important objectives in microelectronics cooling, namely, the reduction of peak temperatures and the attainment of a uniform temperature in a substrate [2,3].

Introduction of particles, which provide nucleation points have been found to enhance the boiling phenomenon in fluids. However, the use of particles in suspended form often affects the fluid flow by producing clogging in flow boiling situations such as those encountered in a heat-pipe wick structure or a micro-heat pipe. As the addition of nanoparticles to produce well-dispersed suspensions (nanofluids) has found to anomalously change most thermophysical properties, it has been recently of great interest to investigate the boiling performance of nanofluids. Some experimental studies on nanofluids have reported a deterioration of performance in pool boiling, and attributed the effect to the deposition of nanoparticles on heating surfaces, thus reducing the surface heat transfer coefficients [4], whereas an increase in critical heat flux values have invariably been noticed [5]. Still, not many studies have been conducted to bring out the variation of the latent heat of vaporization due to the presence of nanoparticles in a liquid medium, which is a problem that requires analysis at the fundamental level, when treated theoretically.

The theoretical work reported in this paper aims at developing a methodology for predicting the enhancement in the latent heat of vaporization of a liquid due to the addition of nanoparticles, using molecular dynamics (MD) simulations. The base fluid chosen for this study is water in which platinum nanoparticles are suspended. This combination was selected for demonstrating the methodology due to the ready availability of the potential functions required in the computational approach, in the literature. However, the methodology can be extended to the case of any material combination, by applying pertinent potentials and other parameters in the simulation.

2 Methodology

Molecular dynamics (MD) [6,7] is one of the most versatile atomistic modeling methods. For simulating the molecular (or atomic, according to the requirements of the problem) interactions at nanoscales, where continuum based methods are not applicable but a quantum mechanical approach is not necessary. MD simulations are based on the equilibrium concepts of classical mechanics, in which the forces between the molecules can be obtained as the spatial derivatives of the characteristic interaction potentials [8]. Various types of potentials are available in the published literature, characterizing the interactions between various similar and dissimilar molecules [8,9,18]. By choosing the appropriate potential which best describes the system under study, various thermophysical properties [10] and thermodynamic quantities of the system can be evaluated using MD simulations. In the present study, the difference in the total energy, as determined from MD simulations, between a system of a saturated liquid and an identical system of saturated vapor under the same conditions of temperature and pressure, is measured as the latent heat of vaporization of the medium.

2.1 Water–Water Interaction

Most of the conventional potential functions used in the case of water, like the extended simple point charge (SPC/E) or Caravetta Clemeni (CC) potential [8], are functions of the distances between the charged particles (positive hydrogen atoms and negative

oxygen atoms). In the present work, the potential used for water was SPC/E [8,9]. The SPC/E potential employs the rigid water configuration, with the distance of OH as 0.1 nm and the angle of HOH, the tetrahedral angle, 104.47°. The effective pair potentials of molecules are expressed as the superposition of van der Waal's potential for the oxygen–oxygen interaction and the electrostatic potential due to charges on oxygen and hydrogen as follows:

$$\phi_{12}(R_1, R_2) = 4\varepsilon_{00}\left[\left(\frac{\sigma_{00}}{R_{12}}\right)^{12} - \left(\frac{\sigma_{00}}{R_{12}}\right)^{6}\right] + \sum_i \sum_j \frac{q_i q_j}{4\pi\varepsilon_0 r_{ij}} \tag{1}$$

In Eq. 1, R_{12} represents the distance between the oxygen atoms, and σ_{00} and ε_{00} are Lennard–Jones parameters. The Coulombic interaction is the sum of nine pairs of point charges. The values of σ_{00} and ε_{00} are given in the literature [8] as 0.3166 nm and 1.0797×10^{-21} J, respectively.

2.2 Water–Platinum Interaction

The potential proposed by Spohr and Heinzinger [11] was used to model the water–platinum interaction, as suggested and used by Kimura and Maruyama [12], for the study of a water droplet on a platinum surface. The potential for the water–platinum interaction is the sum of three potential functions as given by the set of equations [12]:

$$\begin{aligned}
\phi_{H_2O-Pt} &= \phi_{O-Pt}(\gamma_{OPt}, \rho_{OPt}) + \phi_{H-Pt}(\gamma_{H_1Pt}) + \phi_{H-Pt}(\gamma_{H_2Pt}) \\
\phi_{O-Pt} &= \left[a_1 e^{(-b_1 r)} - a_2 e^{(-b_2 r)}\right] f(\rho) + a_3 e^{(-b_3 r)} [1 - f(\rho)] \\
\phi_{H-Pt} &= a_4 e^{(-b_4 r)} \\
f(\rho) &= e^{(-c\rho^2)} \\
a_1 &= 1.8942 \times 10^{-16}\ \text{J}, \quad b_1 = 11.004\ \text{nm}^{-1} \\
a_2 &= 1.8863 \times 10^{-16}\ \text{J}, \quad b_2 = 10.996\ \text{nm}^{-1} \\
a_3 &= 10^{-13}\ \text{J}, \quad b_3 = 53.568\ \text{nm}^{-1} \\
a_4 &= 1.742 \times 10^{-19}\ \text{J}, \quad b_4 = 12.777\ \text{nm}^{-1} \\
c &= 11.004\ \text{nm}^{-1}
\end{aligned} \tag{2}$$

The parameter ρ in Eq. 2 is the length of the projection of the distance vector onto the surface plane, as used by Kimura and Maruyama [12]. In the present study, where the simulation cell is three-dimensional, it is justifiable to assume the value of ρ to be same as that of the distance vector.

2.3 Platinum–Platinum Interaction

A crucial aspect of the present work is the modeling of nanoparticles. A nanoparticle is a cluster of several molecules which interact among themselves. The integrity of

a cluster is quite often determined by these interactions. Therefore, it is of primary importance to develop interactions to realistically represent nanoparticles (and hence nanofluids) in the MD simulation. This was incorporated in the present work by considering a nanoparticle as a cluster of molecules of platinum, and applying a cluster potential as will be explained below. This also provides a method for conducting parametric studies to determine the effect of the nanoparticle size on the latent heat enhancement in nanofluids.

A simple two-body LJ potential is assumed for Pt–Pt interactions within a cluster;

$$\phi_{\mathrm{LJ}}(r) = 4\varepsilon\left[\left(\frac{\sigma}{r}\right)^{12} - \left(\frac{\sigma}{r}\right)^{6}\right], \tag{3}$$

where ε and σ are LJ potential parameters which take the values of 65.77 kJ $\cdot$ mol^{-1} and 0.2732 nm, respectively [13]. However, the use of this potential alone will not suffice in ensuring the integrity of the cluster. By integrity, what is implied is that the cluster should not break up into individual Pt atoms during the long MD simulation runs. Therefore, a cluster potential that ensures cluster integrity is employed such that the net potential is given by the sum of the LJ potential and the cluster potential. In the present work, the cluster atoms are assumed to be held together by a finitely extendable nonlinear elastic (FENE) potential [13] which is defined as

$$U_{\mathrm{FENE}} = -A\varepsilon \ln\left[1 - \left(\frac{r}{B\sigma}\right)^{2}\right] \tag{4}$$

For platinum, A and B take the values of 5.625 and 4.95, respectively [13].

The strength of the application of the FENE cluster potential in simulating the nanoparticles will be demonstrated and discussed later, with the help of a cluster stabilization characteristic obtained from the simulation run.

To estimate the diameter of a nanoparticle, the radius of gyration (R_{g}) is required. This is estimated during the simulation using the following relation [14]:

$$R_{\mathrm{g}}^2 = \frac{\sum_{i=1}^{N_{\mathrm{P}}} (r_i - r_{\mathrm{c.m}})^2}{N_{\mathrm{P}}} \tag{5}$$

In the above equation, N_{P} is the number of atoms in the nanoparticle and $r_{\mathrm{c.m}}$ is the position of the center of mass of the nanoparticle. Assuming a homogeneous mass distribution, the effective outer diameter of the nanoparticle, d_{NP}, can be estimated using the following relation [14]:

$$d_{\mathrm{NP}} = \left(\frac{20R_{\mathrm{g}}^2}{3}\right)^{1/2} \tag{6}$$

In the present investigation, simulations have been performed assuming various sizes of the nanoparticle in the suspension, in the range of 0.5 nm to 0.7 nm, in order to study the effect of the particle diameter on the latent heat. However, the major influencing

parameter identified is the volume fraction of nanoparticles in the suspension, and, as will be presented and discussed later, the effect of the volume fraction is found to be much more significant than that of the particle diameter in determining the effective latent heat of the nanofluid.

3 Molecular Dynamics Simulation Details

In the present work, MD simulations are performed in an NPT (constant number, pressure, and temperature) ensemble. In modeling water, the initial configuration assumed is such that all the water molecules are arranged in a simple cubic structure. The unit cell, when extended in all three directions, will form the simulation box for the MD simulation. In the present work, the box consists of 64 water molecules; this simulation box, along with the imposed periodic boundary condition, is used to model the base fluid, water, in the MD simulation. The simulation box length can be determined for a fixed number of particles by calculating the volume of the simulation box from the mass of the water molecules and density of water at the system temperature (the temperature at which phase change takes place). As in the present simulation, MD runs have to be performed with water in both the liquid and the vapor states; the corresponding density values are used in determining the box length in the two states. For the liquid state at a temperature of 300 K and a pressure of 1 bar, the simulation box has a length of 1.259 nm. The simulation box length for the vapor state at the same conditions was 13.67 nm. The time step used was 10^{-17} s. The number of time steps in most simulations was 120 000 which meant that the simulation ran for around 1.2 ps in real time. Random velocities are initially assigned to each molecule based on the system temperature. The velocity of the center of mass is made zero, so that the system does not drift in space, to simulate the pool boiling situation.

In the equilibration process, the system is allowed to evolve into an equilibrium state with the specified temperature and pressure. In the present work, the imposed temperature and pressure were 100 °C and 101.3 kPa, respectively, for the baseline case, which were changed systematically in the parametric study to obtain the variation of latent heat with temperature. The temperature and pressure of the system were controlled using the implementation of a thermostat [9] and a barostat [15], respectively. The "thermostat" is an artificial means by which a system is brought to a desired temperature, by suitably rescaling the velocities during simulation. Similarly, a "barostat" is used to maintain a constant pressure, by rescaling the length of the simulation box by a factor determined based upon the desired pressure at any computational stage. The methodology is explained below.

The temperature was controlled by making use of the following equation [8]:

$$V_{i,j}^{\text{new}} = V_{i,j}^{\text{old}} \sqrt{\frac{T_{\text{required}}}{T_{\text{actual}}}}, \tag{7}$$

where $V_{i,j}^{\text{new}}$is the new velocity of particle "i" in the direction "j"; $V_{i,j}^{\text{old}}$ is the old velocity of particle "i" in the direction of "j"; T_{required} is the required temperature

(here say 100 °C); and T_{actual} is the actual temperature of the system at the instant of computation.

Pressure control in the system was achieved through the equation,

$$\mu = \left[1 - \frac{\beta \Delta t}{\tau_{\text{P}}} (P - P_0)\right]^{\frac{1}{3}}, \tag{8}$$

where μ is the box scaling factor, β is the isothermal compressibility, Δt is the integrating time step, τ_{p} is the barostat time constant [6], P_0 is the required pressure, and P is the computed instantaneous pressure of the system. The barostat is applied by rescaling the simulation box length by multiplying it by the box scaling factor.

The NPT ensemble was maintained using the following methodology. Initially, the box length was maintained a constant and the thermostat is applied. The scaling interval that was employed for the thermostat was 100 time steps. After the temperature was stabilized, the barostat was applied until the pressure also reached a constant value. By trial and error, the best strategy for maintaining an NPT ensemble was to employ a thermostat for the first 100 000 time steps and then to apply the barostat for 20 000 time steps.

The time evolution method used in the computation obtains the positions and velocities of the molecules at successive states of the system, using a time integration algorithm based on the finite difference method [16]. The velocity-Verlet algorithm [9] was used for platinum molecules of the cluster. The equations used in velocity-Verlet algorithm are given below:

$$\begin{aligned} r(t + \Delta t) &= r(t) + v(t)\Delta t + (1/2)a(t)\Delta t^2 \\ v(t + \Delta t/2) &= v(t) + (1/2)a(t)\Delta t^2 \\ a(t + \Delta t) &= -(1/m)\nabla V(r(t + \Delta t)) \\ v(t + \Delta t) &= v(t + \Delta t/2) + (1/2)a(t + \Delta t)\Delta t, \end{aligned} \tag{9}$$

where $r(t)$, $v(t)$, and $a(t)$ represent position, velocity, and acceleration, respectively, at the time instant t.

Unlike atoms which can be treated as spherical particles, the simulation of molecules is complicated by features like rotation and intermolecular bonds. In particular, molecular bonds constrain the motion of the atoms that comprise the molecule. Therefore, methods to integrate the equations of motion of the molecules must also take into account the bond constraints. One of such methods, the RATTLE algorithm [9], was used for the water molecules. The RATTLE algorithm first integrates the equations using the velocity-Verlet algorithm and then corrects the position and velocity of each atom in the molecule so as to maintain the bond length and bond angle constraints. This is accomplished by repeating the following steps:

1. Calculate $r(t + \Delta t)$ in the absence of the constraints (as in Eq. 9).
2. Calculate velocities at mid-step using $v(t + \Delta t) = v(t) + (1/2)a(t)\Delta t$.
3. Start the iterative loop for calculating the Lagrange multipliers, $\lambda_{ij}^{\text{RR}}(t)$.

a. Pick a constraint involving atoms i and j.
b. If the current bond length differs from the fixed bond length d_{ij} by more than the prescribed tolerance, then determine the value of Lagrange multipliers necessary to satisfy the constraint more closely and add this term to $r_i(t+\Delta t)$, $r_j(t+\Delta t)$ and $v_i(t+\Delta t/2)$, $v_j(t+\Delta t/2)$ according to the following equations; otherwise, go back to step 3a and pick a new constraint.

$$r(t+\Delta t) = r(t) + \Delta t v(t) + \frac{1}{2}\Delta t^2 \left[a(t) - \frac{2}{m_i} \sum_j \lambda_{ij}^{\mathrm{RR}}(t) r_{ij}(t) \right] \quad (10)$$

$$v(t+\Delta t) = v(t) + \frac{1}{2}\Delta t \left[a(t) - \frac{2}{m_i} \sum_j \lambda_{ij}^{\mathrm{RR}}(t) r_{ij}(t) + a(t+\Delta t) - \frac{2}{m_i} \sum_j \lambda_{ij}^{\mathrm{RV}}(t+\Delta t) r_{ij}(t+\Delta t) \right] \quad (11)$$

Continue this iterative procedure until all bond constraints are satisfied within the prescribed tolerance.

4. Calculate $a(t+\Delta t)$.
5. Complete the velocity move in the absence of constraints using $v(t+\Delta t) = v(t+\Delta t/2) + (1/2)a(t+\Delta t)\Delta t$.
6. Start the iterative loop for calculating the Lagrange multipliers $\lambda_{ij}^{\mathrm{RV}}(t)$ (change $v(t)$ so that all velocity constraints are satisfied within tolerance).

a. Pick a constraint involving atoms i and j.
b. If the dot product of $r_{ij}(t+\Delta t)$ and $v_{ij}(t+\Delta t)$ differs from zero by more than the prescribed tolerance (chosen as 10^{-6}), then determine the value of $\lambda_{ij}^{\mathrm{RV}}(t+\Delta t)$ necessary to satisfy the velocity constraint more closely and add this term, according to Eq. 11; otherwise, go back to step 6a and pick a new constraint.

The iterative procedure is continued until all velocity constraints are satisfied within the prescribed tolerance.

Platinum nanoparticles were introduced (in the form of clusters of atoms) into the simulation box to simulate the nanofluid. The initial arrangement of platinum atoms in these clusters can be of any convenient form, depending on the number of atoms in a cluster, representing the particle size. For instance, it could be taken as a simple cubic structure if there are eight atoms in a cluster. Each atom in the cluster was assigned the same velocity based on the system temperature.

The characteristic property of the system to be determined from the MD simulation is its total energy. As mentioned earlier, the latent heat of vaporization can be calculated from the total energy of the system after and before the phase-change phenomenon. The total energy of the system is the sum of the kinetic and potential energy components and is given by the expression,

$$e = \sum_j \frac{1}{2} m_j v_j^2 + \sum_j \sum_{i \neq j} \phi_{ij}, \tag{12}$$

where m_j is the mass and v_j is the velocity of the jth particle.

The evaluation of the latent heat of vaporization requires two MD simulations. In the first one, liquid water at the prescribed saturation condition (100 °C and 101.3 kPa for the baseline case) is simulated and the total energy of the system is determined. In the second simulation, water vapor at the same condition is modeled and the total energy calculated. The difference in the energy gives the amount of energy required to convert the system from liquid water to water vapor, i.e., the latent heat of vaporization at the specified temperature.

C++ programs were developed for simulation of the pure base fluid (water) and the platinum–water nanofluid. Simulations were first carried out to investigate the variation of the latent heat of water with pressure, which served to validate the proposed methodology by comparing the results with standard values, as will be presented later in Fig. 5. Then, the nanoparticle suspensions were simulated and the variation of the latent heat with the volume fraction of nanoparticles was obtained. This parametric study was the basic objective of the present investigation, which gave the change in latent heat of the base fluid due to the addition of nanoparticles.

4 Experimental Study

Experiments have been conducted in order to determine the latent heat of the nanofluid, and thus to obtain the enhancement due to the addition of the nanoparticles in water. The results from these experiments were compared with the simulation results to benchmark the MD simulation. However, the nanoparticles used in the experimental study were of aluminum oxide, and the comparisons were more of a qualitative nature, on the trends of latent heat enhancement with respect to the volume fraction. Still, the trends and variations obtained were found to agree very well with the simulation results, which indicated that the order of magnitude of the latent heat enhancement is not much affected by the type of the nanoparticle. The comparative studies will be presented and discussed later in this paper.

Nanofluids of various volume fractions (0.005, 0.01, and 0.02) were prepared using an ultrasonic agitation process, using aluminum oxide nanoparticles in water. In the experimental procedure, the nanofluid was boiled in an open vessel, while supplying electrical heat such that all the heat was dissipated into the fluid. The mass loss in the nanofluid over a given time during the boiling process, measured using a highly sensitive electronic balance, was used for determining the latent heat of vaporization.

$$\text{Latent heat } h_{\text{fg}} = \frac{VIt}{\Delta m}, \tag{13}$$

where V and I are the input current and voltage for the heater, t is the time of observation, and Δm is the loss of mass during this time.

5 Results and Discussion

Figure 1 represents the stabilization of a nanoparticle cluster, through a plot between the effective cluster diameter with respect to the number of time steps during the evolution. The simulation was used to study and demonstrate the strength of the cluster potential used in the computation. A nanoparticle containing four platinum atoms in a simulation box containing 64 water molecules was used for this simulation. As is clear from the graph, the effective diameter of the cluster converges to a constant value within 50 time steps. This result indicates that the FENE cluster potential used in the present simulation is quite effective in modeling the nanoparticle.

Figure 2 shows the temperature variation during the equilibration process in a typical run of the MD simulation. The temperature is found to reach the stabilized equilibrium value within around 2500 time steps, due to the use of a very effective thermostat in the simulation, as explained before.

Before using the MD code for evaluating the latent heat characteristics of the nanofluid, it was benchmarked using the well-established pressure–density relation for steam. The results obtained from the simulation were compared with the values from

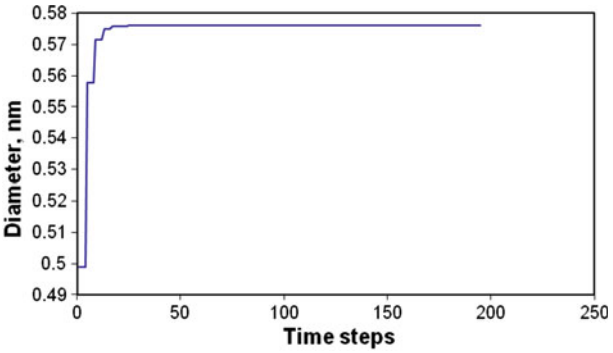

Fig. 1 Stabilization of a cluster of four platinum atoms in water

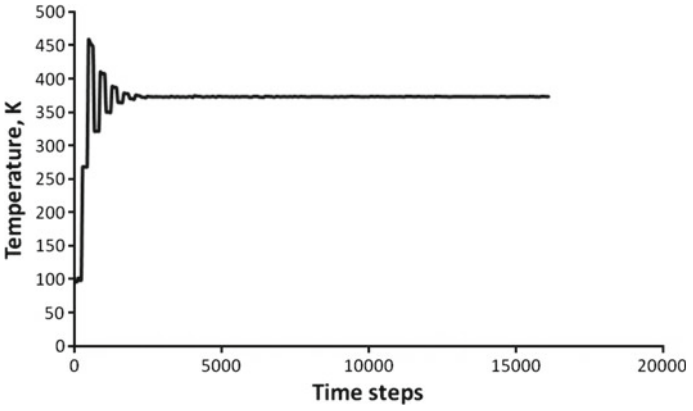

Fig. 2 Typical temperature variation during the equilibration process

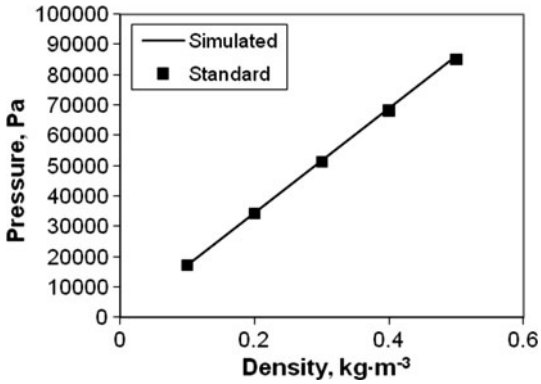

Fig. 3 Pressure–density plot for steam at 373 K, comparing simulated and standard values

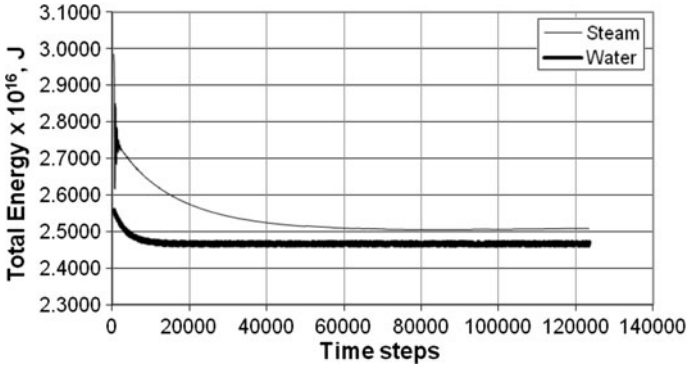

Fig. 4 Determination of the latent heat in a typical case analyzed. The difference between the two curves at convergence gives the latent heat value

standard steam tables [17] as shown in Fig. 3. The computed values are seen to be in very good agreement with the standard values, as is clear from the graph.

Figure 4 depicts the procedure for determining the latent heat of vaporization of water from the difference in total energies of vapor and liquid states at 100 °C and 101.3 kPa (1 atm.). It is found that in around 80 000 time steps, the difference in total energies converges to a constant value, which is measured as the latent heat of vaporization of the medium at the given condition.

The comparison of the latent-heat values of water as obtained from the MD simulations with standard values [17] is given in Fig. 5. The values are found to agree reasonably well, both in the magnitude of the values and the variation with respect to the pressure, which, along with the result presented in Fig. 3, validates the present computational methodology within a good accuracy limit. The maximum and minimum errors resulting from the simulations for pure water (shown in Fig. 5), as compared with the available standard value have been estimated as $56\,\mathrm{kJ}\cdot\mathrm{kg}^{-1}$ and $63\,\mathrm{kJ}\cdot\mathrm{kg}^{-1}$, which translates to a maximum error limit of $\pm 3\,\%$ for the simulation. The characteristic decrease in the latent heat of vaporization of water with an increase in the pressure is also captured correctly by the simulation.

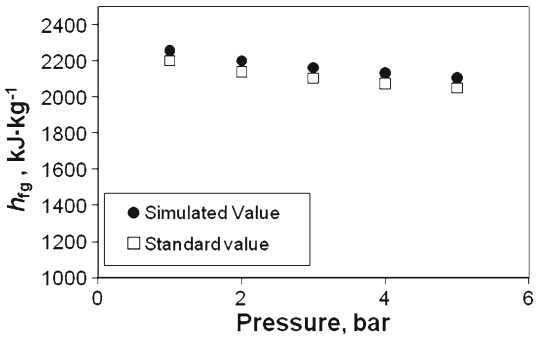

Fig. 5 Variation of the latent heat of vaporization of water with the saturation pressure

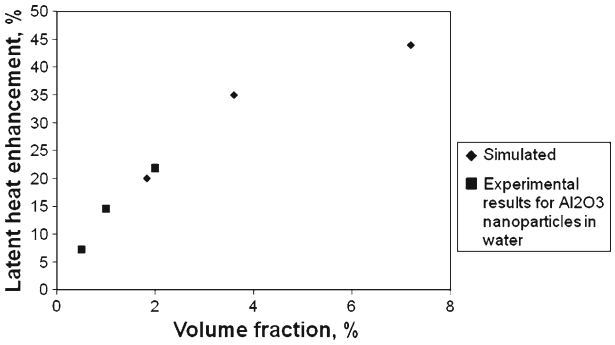

Fig. 6 Latent heat enhancement as a function of the volume fraction of nanoparticles, for a simulation of the Pt nanofluids with a particle size of 0.5 nm, compared with experimental data for Al_2O_3 nanofluids with 20 nm sized particles

A typical result on the enhancement of the latent heat due to the addition of nanoparticles of a particular size, with different volume fractions, computed by MD simulation, is plotted in Fig. 6. For a qualitative comparison of the results of the MD simulations in the case of water–platinum nanofluids of various volume fractions, they are shown along with experimental results on a water–Al_2O_3 system. The enhancement of the latent heat in nanofluids could possibly be attributed to the introduction of the action of extra bonds between the molecules of the base fluid, brought in by the nanoparticles. This will require extra energy to break the new bonds during the phase change, leading to an increase in the latent heat. Though the differences due to the use of a different material (aluminum oxide) and a different particle size in the experimental study are seen in the graph, the trend of variation predicted by the computational simulations is found to match very well with the experimental results. Further, it is interesting to note that the values are quantitatively also similar, implying that the influences of the nanoparticle material and size are apparently smaller compared to that of the volume fraction. However, extensive investigations would be required to make conclusive observations in this regard.

Figure 7 shows a typical result on the variation in the predicted enhancement of latent heat with the nanoparticle size, for a fixed volume fraction. A decreasing trend is observed in the latent-heat value with an increase in the nanoparticle size. This could

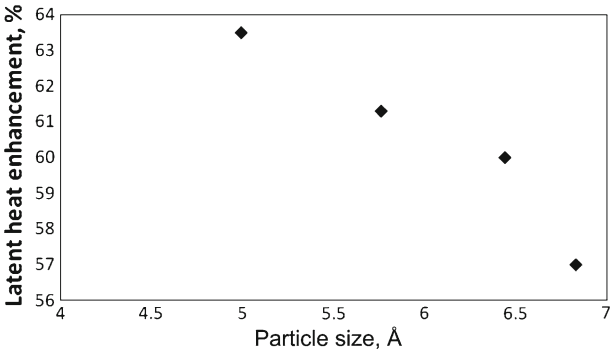

Fig. 7 Latent heat enhancement as a function of the nanoparticle size, for volume fraction of 10.8 %

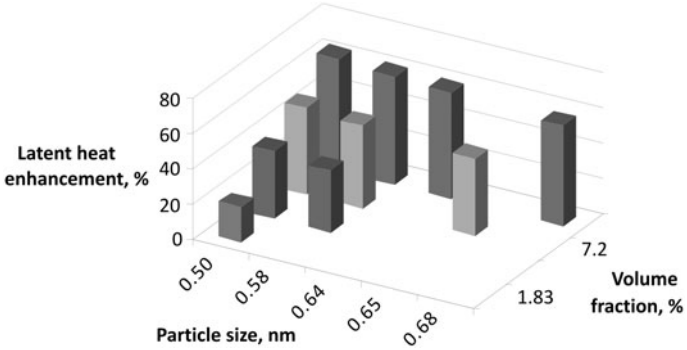

Fig. 8 Variation in the enhancement of latent heat of vaporization with the volume fraction and the nanoparticle size

be attributed to the fact that the surface-to-volume ratio of the nanoparticles increases with a decrease in the particle size at fixed volume fraction. The particle size was varied by changing the number of platinum molecules in the cluster, and the volume fraction was changed by changing the number of nanoparticles in the simulation box.

The combined effect of the size and volume fraction of nanoparticles on the enhancement in the latent heat of vaporization, as predicted by the MD simulations, is shown in Fig. 8. It is found that the change in the volume fraction has a predominant effect on the enhancement compared to the effect of the particle size.

6 Conclusions

An investigation based on MD simulation has been presented in this paper, in order to predict the enhancement of the latent heat of vaporization of a base fluid due to the suspension of nanoparticles. A general methodology has been developed and demonstrated in predicting and performing parametric studies in the case of a water–platinum system, to a very good degree of accuracy within practical application limits.

An enhancement in the latent heat is noticed in nanofluids, which is found to increase with an increase in the volume fraction and with a decrease in the size of the nanoparticles. Both the computational and experimental results on nanoparticle suspensions show a similar qualitative nature. The effect of the volume fraction in the enhancement of the latent heat is found to be more pronounced than the effect of the particle size.

The methodology presented in this work is found to be effective in evaluating the modification in the latent heat of nanofluids, with a change in volume fraction and size of nanoparticles, and can be utilized in obtaining optimum combinations of these parameters. This method can also be extended to capture the effects of agglomeration of nanoparticles on the latent heat of vaporization of nanofluids. Although the volume fraction used in the MD simulations are small (0.005 to 0.02), it is still possible that, during the simulations, the platinum nanoparticles could meet each other and might aggregate to form bigger clusters. The effect of agglomeration could be incorporated into the present model by including cluster–cluster interactions [10,13]. However, it should also be noted that further modifications could be incorporated in the simulation model, to overcome the idealizations and simplifications of the potential functions used, and by incorporating a larger number of molecules in the simulation, thus refining and fine-tuning the modeling methodology.

Acknowledgment The authors gratefully acknowledge the Technical Quality Improvement Program (TEQIP) of the Government of India, for providing the computational and experimental facilities at the Nanotechnology Research Laboratory (Center for Nanotechnology), National Institute of Technology, Calicut, India.

References

1. G.P. Peterson, C.B. Sobhan, Applications of Microscale Phase Change Heat Transfer: Micro Heat Pipes and Micro Heat Spreaders, in *Handbook of Microelectromechanical Systems*, ed. by M. Gad-el-Hak (Taylor and Francis/CRC Press, Boca Raton, FL, 2006)
2. C.B. Sobhan, S.V. Garimella, Microscale Thermophys. Eng. **5**, 293 (2001)
3. S.V. Garimella, C.B. Sobhan, Annu. Rev. Heat Transf. **13**, 1 (2003)
4. S.K. Das, N. Putra, W. Roetzel, Int. J. Heat Mass Transf. **46**, 851 (2003)
5. H. Kim, J. Kim, M.H. Kim, Int. J. Heat Mass Transf. **49**, 5070 (2006)
6. D.C. Rappaport, *The Art of Molecular Dynamics Simulation*, 2nd edn. (Cambridge University Press, Cambridge, 2004)
7. C.B. Sobhan, G.P. Peterson, *Microscale and Nanoscale Heat Transfer—Fundamentals and Engineering Applications* (Taylor and Francis/CRC Press, Boca Raton, FL, 2008)
8. S. Maruyama, Adv. Numer. Heat Transf. **2**, 189 (2000)
9. R.J. Sadus, *Molecular Simulation of Fluids: Theory, Algorithm and Object Orientation* (Elsevier, Amsterdam, 1999)
10. N. Sankar, N. Mathew, C.B. Sobhan, Int. Commun. Heat Mass Transf. **35**, 867 (2008)
11. E. Spohr, K. Heinzinger, Ber. Bunsen-Ges. Phys. Chem. **92**, 1358 (1988)
12. T. Kimura, S. Maruyama, Microscale Thermophys. Eng. **6**, 3 (2002)
13. J. Eapen, Ph. D. Dissertation, MIT, Boston, 2006
14. G. Galliero, S. Volz, J. Chem. Phys. **128**, 064505 (2008)
15. H.J.C. Berendsen, J.P.M. Postma, W.F.V. Gunsteren, A.D. Nola, J.R. Haak, J. Chem. Phys. **81**, 3684 (1984)
16. M.P. Allen, D.J. Tildesley, *Computer Simulation of Liquids* (Clarendon Press, Oxford, 1987)
17. *ASME Steam Tables*, American Society of Mechanical Engineers (2006)
18. A. Rahman, F.H. Stillinger, J. Chem. Phys. **55**, 3336 (1971)